Int. J. Electrochem. Sci., 7 **(2012)** 9441 - 9453

International Journal of
ELECTROCHEMICAL
SCIENCE
www.electrochemsci.org

Reactivities of Modified and Unmodified Exfoliated Graphite Electrodes in Selected Redox Systems

T. Ndlovu[1], *O.A. Arotiba*[1,*], *S. Sampath*[1,2], *R.W. Krause*[1] *and B.B. Mamba*[1]

[1] Department of Applied Chemistry, University of Johannesburg, PO Box 17011, Doornfontein 2028, Johannesburg, South Africa,
[2] Indian Institute of Science, Department of Inorganic and Physical Chemistry, Bangalore, 560012, India
[*]E-mail: oarotiba@uj.ac.za

Received: 10 July 2012 / *Accepted:* 30 August 2012 / *Published:* 1 October 2012

The electrochemical profiles of exfoliated graphite electrodes (EG) and glassy carbon electrodes (GCE) were recorded using cyclic voltammetry and square wave voltammetry in the presence of various supporting electrolytes and $[Fe(CN)_6]^{3-/4-}$, $[Ru(NH_3)_6]^{2+/3+}$,ferrocene redox probes. In the supporting electrolytes (KCl, H_2SO_4, NaOH, tetrabutylammoniumtetraflouroborate, phosphate buffers), the potential windows of EG were found in some cases to be about 200 mV larger than that of GCE. The electroactive surface area of EG was estimated to be 19.5 % larger than the GCE which resulted in higher peak currents on the EG electrode. Furthermore, EG was modified with various nanomaterials such as poly (propylene imine) dendrimer, gold nanoparticles, and dendrimer–gold nanoparticles composite. The morphologies of the modified electrodes were studied using scanning electron microscopy and their electrochemical reactivities in the three redox probes were investigated. The current and the reversibility of redox probes were enhanced with the presence of modifiers in different degrees with dendrimer and gold nanoparticles having a favorable edge.

Keywords: Exfoliated graphite electrode, electrode modification, glassy carbon electrode, redox probe, dendrimer, gold nanoparticles

1. INTRODUCTION

A wide range of electrodes such as Pt, Au, C, Hg amalgams and semiconductors (such as indium-tin oxide) have been reported in electrochemistry based research [1]. As plausible as these electrodes have been in terms of application, continuous efforts are still being made to improve their performance by using them in the modified forms. For example, traditional electrodes have been modified with polymers, dendrimers, nanoparticles, organic molecules for a wide range of applications

such as bioelectronics, catalysis, sensors (biomedical, chemical or biological) and biosensors owing to their enhanced properties which may be conductivity, electrocatalysis, biocompatibility, potential robustness etc [2,3]. Aside the art of modification of electrode, electrochemists also quest for new electrode materials which may be another form of the existing ones. For example boron doped diamond electrode, pyrolytic graphite, or an entirely new element e.g. silicon. Generally, carbon based electrodes seem to be the most commonly used electrodes and also have the highest number of varieties which include glassy carbon, carbon paste, carbon fibre, carbon pencil, pyrolytic graphite and exfoliated graphite.

Exfoliated graphite is a very low density form of carbon that results from the exfoliation of intercalated graphite at high temperature [4]. This puffed carbon is mechanically interlocked by high pressure compression to form a resilient sheet known as flexible graphite [4,5]. The recompressed material exhibits high temperature resistance, good electrical conductivity, high porosity with a high surface area compared to other graphitic materials [6]. The flexibility, ease of shaping, and the unusual microstructure (compared to other forms of carbon) suggest possible attraction for the use of exfoliated graphite as an electrode material in batteries, in electrolysis and in chemical sensors [7].

Glassy carbon is a form of carbon that is extremely hard and highly conductive to electrons, and is thus a good choice for fabricating inert electrodes [8,9]. Compared to EG, GCE is more expensive, more difficult to shape and fabricate into an electrode [8]. Although GCE is fairly unreactive, it can form strong covalent bonds on modification with typical functional groups such as the amine group (to form C-N). Such strong bonds make it difficult to clean as opposed to EG where the surface is renewed upon polishing owing to its lubricating layered structure. This cleaning process is more effective compared to the chemically aggressive cleaning methods applied to GCEs. Based on the highlighted advantages of EG over GCE, it will be worthwhile to explore its electrochemical properties vis a vis GCE.

There are a number of redox systems that have been used to describe and explain the electron-transfer kinetics on carbon-electrodes based on the electrochemical reversibility. There are quasi-reversible inorganic systems and quasi-reversible organic systems [10]. For example, the electrochemistry of $[Fe(CN)_6]^{3-/4-}$ redox probe has been extensively studied and used to benchmark various electrodes such as GCE[10]. However electrochemical data on the potential window of EG in common electrolytes and the reactivities of redox systems at the EG interface are not available. Also, while a myriad of reports on modified GCE and their application exist, similar reports based on EG are scanty. For example GCE have been modified with a number of nanomaterials such as gold nanoparticles (AuNP) [11,12], cobalt oxide (CoO) [2,13], silver nanoparticles (AgNP) [14,15], bismuth (Bi) [16,17] and poly(propylene imine) dendrimer (PPI) [18,19]. AgNP modifier have been used successfully for the detection of Cr(VI) with increased sensitivity [15] while bismuth has been deposited onto GCE and carbon paste electrodes for the detection of a number of heavy metals with very low detection limits [17,20,21]. Many kinds of nanoparticles, including metal nanoparticles, oxide nanoparticles, and even composite nanoparticles, have been widely used in GCE based electrochemical sensors and biosensors [22].

We therefore report on the electrochemical characterization of the EG electrode using cyclic voltammetry and square wave voltammetry in known electrolytes and redox systems. In this study, a

comparison of GCE and EG was extensively carried out on all the used electrolytes. In addition, the electrochemical behaviours and morphologies of modified EG electrodes were examined.

2. EXPERIMENTAL

2.1. Reagents and instruments

Generation 2 (G2) poly(propylene imine) (PPI) dendrimer was purchased from SyMO-Chem, Eindhoven, Netherlands. All other chemicals such as natural graphite, $HAuCl_4$, KCl, H_2SO_4, HNO_3, $K_3Fe(CN)_6$, $K_4Fe(CN)_6$, $Ru(NH_3)_6Cl_3$, $Ru(NH_3)_6Cl_2$, ferrocene, KH_2PO_4, K_2HPO_4, HCl, KOH and others were obtained from Sigma Aldrich and were used as purchased. Ultra pure water from Millipore was used to prepare all solutions. All electrochemical measurements were done on an Autolab PGSTAT 302N using a three-electrode configuration. GCE and EG (3 mm diameters) were used as working electrodes while counter electrode and reference electrode were platinum wire, and Ag/AgCl (3M Cl^-) respectively. Scanning Electron Microscopy (SEM) was used to probe the surface morphology of the electrodes.

2.2. Fabrication procedure for EG electrodes

The EG was prepared according to a reported procedure [23]. The resultant EG particles were restacked without any binder to form pellets/sheets by compressing approximately 1 g of EG at a pressure of 58 kPa for 6 hours. Electrodes (5 mm diameter) were then fabricated from these pellets using conducting silver paint and copper wire [22].

2.3. Electrode modification

For the modification of the EG electrode (5 mm diameter) with generation 2 poly(propylene imine) (PPI) and gold nanoparticles (AuNP), the procedure reported by Arotiba et al. [12] was used. Briefly, a 10 mM solution of G2 PPI in 0.1 M phosphate buffer solution (pH 7) was used for the electrodeposition of PPI onto the EG electrode surface by cycling the potential from -400 mV to 1100 mV for 10 cycles at a scan rate 50 mV s^{-1}. The PPI modified EG electrode was referred to as EG-PPI. For the modification of EG with AuNP, the same procedure was employed using a 5 mM solution of $HAuCl_4$ (without PPI) and this electrode was referred to as EG-AuNP. A nanocomposite of PPI and AuNP was electro-co-deposited onto the electrode surface using equal amounts of the PPI and $HAuCl_4$ solutions and the resultant electrode was referred to as EG-PPI-AuNP.

All the modified electrodes were electrochemically characterized using cyclic voltammetry (CV) and square wave voltammetry (SWV) in 5 mM mixture of $K_4[Fe(CN)_6]/K_3[Fe(CN)_6]$ and 1 mM mixture of $Ru(NH_3)_6Cl_3/Ru(NH_3)_6Cl_2$ ($(Ru(NH_3)_6]^{+2/+3}$) in 0.1 M KCl as the supporting electrolyte and in5 mMferrocene (dissolved in acetonitrile containing 0.1 M tetrabutylammoniumtetraflouroborate (TBATFB))

3. RESULTS AND DISCUSSION

3.1.Characterization of EG using SEM

Natural graphite has a flake-like structure (Fig 1a) and the average particle size was between 400-500 μm. Particles smaller than 300 μm have been reported to cause intercalates to mainly desorb on the edges, and hence no expansion occurs [24]. Evidence of an increase in the distance between the layers in graphite was visible in GIC (Fig 1b). This demonstrates that the bisulphate ions were intercalated into the graphite layers resulting in an increase in the *c*-axis distance. The exposure of GIC to high temperatures gives rise to sudden vaporization of the intercalates (a process called exfoliation), resulting in an accordion-like structure with a greater increase in the *c*-axis distance (Fig 1c). Celzard et al. reported that an increase in length of up to 300 times of the initial length is possible, while the diameter remains unchanged [24]. This results in an increase in the volume of the material. This is because during exfoliation, the sudden and intense temperature increase leads to the vaporisation and violent expulsion of the bisulphate ions, resulting in the separation of the layers, an observation also made by Ramesh and Sampath [10].

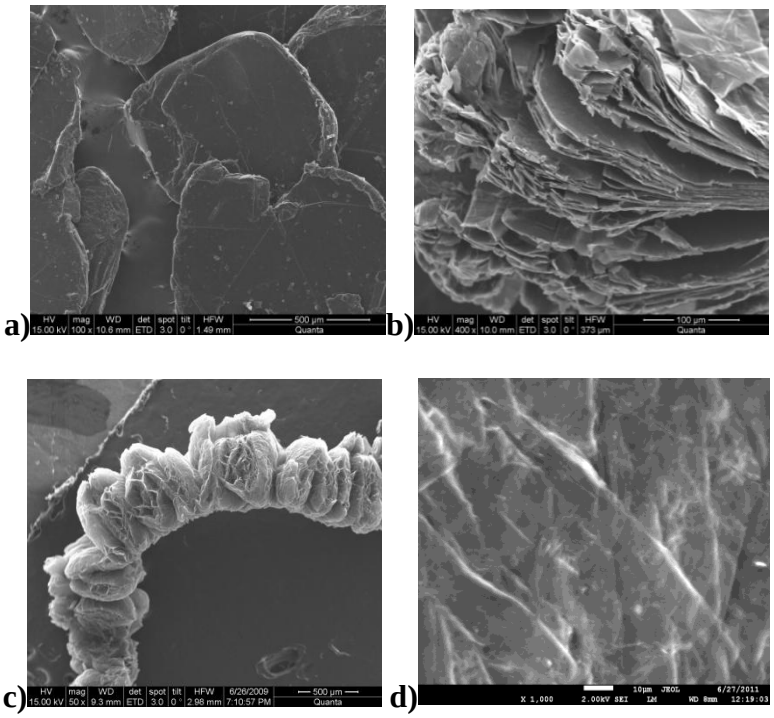

Figure 1. SEM images for **a)** natural graphite, **b)** graphite intecalated compound, **c)** worm-like structure of exfoliated graphite, **d)** recompressed exfoliated graphite

The accordion like structure of EG disappeared after recompression as shown in **Figure 1d,** similar to earlier reports [23]. This disappearance is due to the mechanical interlocking of the layers of EG after recompression leaving behind the basal plane which is pristine recompressed EG without any

attachment or surface modification. The compressed EG was used to fabricate the EG electrodes as described in our earlier work [25].

3.2. Electrochemical characterization: EG vs. GCE

3.2.1. Potential window

Information about the potential window of an electrode in a particular electrolyte, determines to a large extent, its application during electroanalysis. Such knowledge informs whether a particular analyte can be studied without interferences from the oxidation and reduction of the electrode itself or impurities in the electrolyte (and even the electrolyte components) [26]. A wider potential window indicates the possibility of studying a wider range of analytes. The potential window of EG versus GCE was investigated in different electrolytes namely 0.1 M KCl, 0.1 H_2SO_4, 0.1 M NaOH, 0.1 M phosphate buffer (pH 7) and 0.1 M TBATFB in acetonitrile. Figure 2 shows the potential windows for the GCE and EG electrodes in phosphate buffer solution (PBS) at pH 7. The EG electrode had higher capacitive or charging current than the GCE as shown in Figure 2b inset. According to Frysz et al., high capacitance is often associated with high surface roughness and high concentration of oxygen-containing functional groups [27].

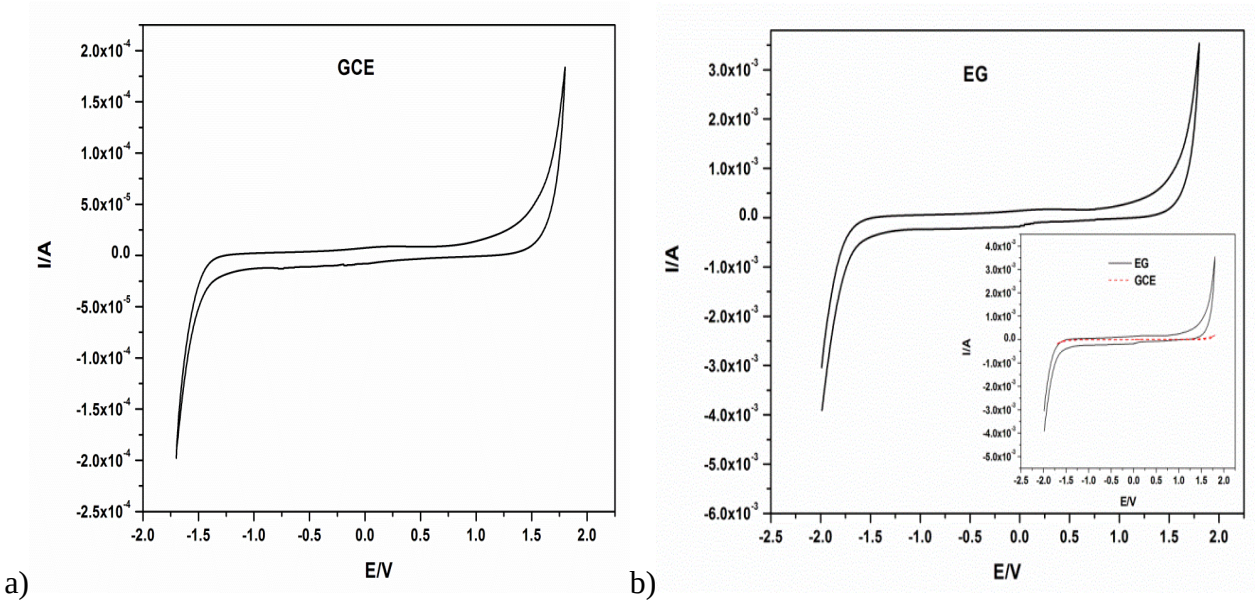

a) b)

Figure 2. CVs showing the potential window of **a)** GCE and **b)** EG electrodes in 0.1 M PBS. Inset in (b) show an overlay of the two voltammograms.

Table 1 shows a summary of the potential windows obtained from some selected supporting electrolytes.

Table 1. Potential windows for EG and GCE in different electrolytes.

Electrolyte	EG	GCE
H_2SO_4	-0.7 to 1.5 V	-0.7 to 1.3 V
NaOH	-1.5 to 0.8 V	-1.7 to 0.8 V
TBATFB	-2.0 to 1.8 V	-1.8 to 1.8 V
Phosphate buffer	-1.6 to 1.3 V	-1.4 to 1.3 V
KCl	-1.6 to 1.3 V	-1.7 to 1.2 V

From Table 1, it is evident that EG and GCE have comparable potential windows and even larger windows (for EG) in some cases. For example in phosphate buffer (pH 7), EG shows a larger potential window of 200 mV at the cathodic end than GCE. This presents a wider potential window for studies that may involve biomaterials, where phosphate buffer pH 7 is generally used as the supporting electrolytes. These findings suggest that the EG electrode may be used for electrochemical measurements instead of the GCE. However, the background or charging currents in EG electrodes were much higher than in GCE in all the electrolytes suggesting the capacitive nature of EG. Depending on the application this capacitive behaviour may be an advantage or disadvantage.

3.2.2. Reactivities in redox systems

The electrochemical behaviours of EG and GCE were also investigated using cyclic voltammetry (CV) and square wave voltammetry (SWV) in selected redox systems. The supporting electrolyte for $[Fe(CN)_6]^{3-/4-}$ and $[Ru(NH_3)_6]^{2+/3+}$ was 0.1 KCl (aqueous) while that of ferrocene was acetonitrile containing 0.1 M TBATFB. Figure 3a shows a comparison of EG and GCE in the different redox systems. EG gave current increases of up to 40% higher anodic and cathodic currents than GCE in all the redox probes. This was due to the greater electroactive surface area for EG compared to GCE.

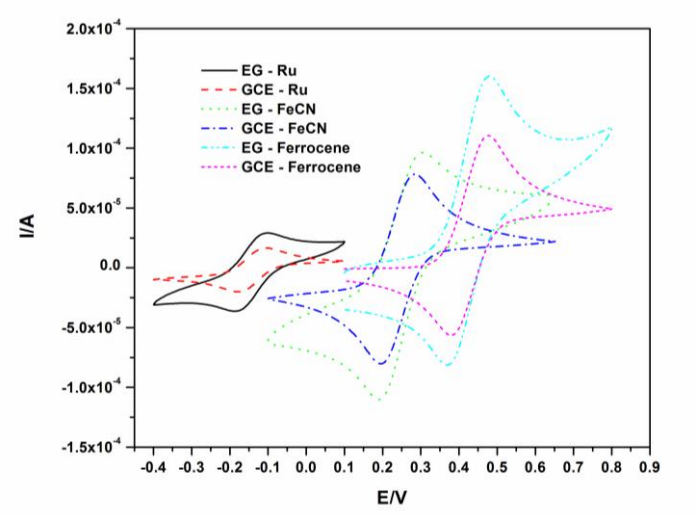

a)

b)

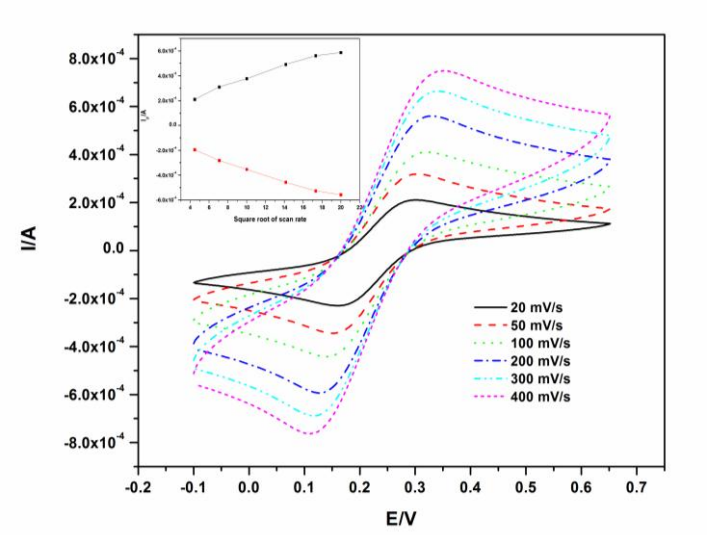

Figure 3. a) A comparison of EG and GCE in the different redox systems using cyclic voltammetry at a scan rate of 50 mV/s **b)** CVs of $[Fe(CN)_6]^{3-/4-}$ in 0.1 M KCl at a bare EG electrode at different scan rates. Inset shows the linear plot of E_{pa} vs. square root of scan rate.

The electroactive surface area (A) of an electrode can be estimated from the slope of the Randles-Sevcik plot described by eqn 1.

$$i_p = 2.69 \times 10^5 n^{3/2} v^{1/2} D^{1/2} AC \quad (1)$$

Where n is the number of electrons, v is the scan rate, D is the diffusion coefficient ($cm^2\ s^{-1}$) A the area of the electrode and C is the concentration in mol L^{-1}. The electroactive area obtained (from $[Fe(CN)_6]^{3-/4-}$) by this method is related to the amount of electroactive sites for each electrode, that is, the area that effectively transfers the charge to the species in solution [28]. The calculated electroactive surface area for EG was 3.92 mm^2, which was 19.5 % higher than for GCE (3.28 mm^2). The larger electroactive surface area on the EG electrode justifies the higher peak currents obtained from the EG electrode over GCE. The EG electrode is also a porous electrode since the compressed EG material has a pore volume of 0.046 $cm^3\ g^{-1}$. Frysz et al reported that porous carbons consist of a continuous matrix of carbon within which is distributed a series of connected open pores [27]. Electrochemical processes are said to occur at the carbon spaces rather than at the outer planar surface resulting in a three-dimensional electrochemical activity rather than the planar responses characteristic to solid electrodes [27]. Coupled with the high surface area, this could be the reasons why higher peak currents were observed for EG.

The kinetic and reversibility properties of electrochemical processes strongly depend on the surface of the electrodes [27]. Hence differences in the surface functional groups, surface crystallographic structure and surface roughness may result in differences in electrochemical behaviour. The electrochemical performance of an electrode can be investigated using CV where the peak separation (ΔE) gives information about the reversibility of the electrochemical process. The peak separation for a reversible process is given by;

$$\Delta E_p = E_{pa} - E_{pc} = \frac{0.059}{n}$$

For a quasi-reversible process ΔE is greater than 0.059/n V while for an irreversible reaction, only a single peak will be observed on one of the potential scans [29]. For systems which show sluggish electron exchange, the peaks are reduced in size and widely separated. For EG and GCE, ΔE was larger than the expected 59 mV, suggesting that the electrochemical reactions were quasi-reversible on both electrodes as shown in Table 2.

Table 2. ΔE values (in mV) obtained from the different redox systems using EG and GCE.

Electrode	$[Fe(CN)_6]^{3-/4-}$	$[Ru(NH_3)_6]^{2+/3+}$	Ferrocene
EG	113	85	107
GCE	90	74	97

For GCE, the ΔE values were smaller and closer to 59 mV in all three redox probes compared to the EG electrode. This implies that electron transfer is faster on the GCE than on the EG electrode interface hence better reversibility. This could be because GCE is compact while the porosity of EG could be delaying the kinetics (adsorption/desorption) at the electrode surface. Another reason could be the fact that the EG electrode used was polished before use hence it had predominantly basal planes which leads to a slow electron transfer. A rough EG electrode surface consists of more edge planes which have been reported to lead to faster electron transfer [10]. The improvement in the electrochemical kinetics on an edge plane has been attributed to the high oxygen/carbon (O/C) ratio as compared to that observed on a basal plane [10]. This is because oxygen containing functional groups were introduced during the preparation stage, especially on the edge planes. The fabricated EG electrode showed quasi-reversibility with ΔE values not more than 25 mV greater than those obtained from GCE. The peak current ratio was almost unity (0.957 (EG) and 0.961 (GCE) in $[Fe(CN)_6]^{3-/4-}$) supporting that the electrochemical reactions were quasi-reversible on both these carbon based electrodes except in ferrocene, which had a lower ratio. This is due to the adsorptive nature of this organic molecule on the sp^2 hybridized EG electrode.

On the bare EG electrode, the CVs of $[Fe(CN)_6]^{3-/4-}$, $[Ru(NH_3)_6]^{2+/3+}$ and ferrocene were recorded at different scan rates between 20 mV/s and 400 mV/s. It was observed that the peak currents of both peaks (oxidation and reduction) increased linearly with the square root of the scan rate as exemplified in Figure 3b (using $[Fe(CN)_6]^{3-/4-}$) with R^2 value of above 0.992. This behaviour is consistent with the observation when using the GCE. These results indicated that the electrochemical kinetics signified a diffusion-controlled process (from the Randle-Sevcik equation) rather than a surface-controlled process at the different scan rates for all the three redox systems. This is an ideal situation for quantitative analyses in practical applications.

These similarities in behaviour (potential windows, faradaic currents, redox behaviour and diffusion coefficients) between EG and GCE suggest that the EG electrode can be used in most

applications where the GCE is used but the EG is more advantageous to use because of its lower costs and higher currents due to a greater surface area.

In general, a material should have the following properties so as to have applicability as an electrode in electrochemistry: i) the material must have electrical conductivity without which electrochemical measurements are not possible; ii) the ability to permit interfacial reactions (kinetics and diffusion controlled phenomena); iii) it must be chemically inert (within a certain potential) so as not to interfere in the interfacial electrochemical reaction; iv) amenability to cleaning and reuse without compromising its electrochemical performance and v) the material as an electrode should lend itself to electrode modification (the modifier can be used to tailor the electrodes for various uses such as encapsulating enzyme in a biosensor).

The electrochemical properties of EG (which were similar or sometimes superior to that of GCE) as a viable electrode as discussed in Section 3.2.1 and 3.2.2, to a large extent have corroborated points (i) to (iv) above. We therefore went further to study the amenability of EG to electrode modification (point (v)) and its behaviour as a modified electrode. The chosen modifiers were AuNP and PPI dendrimer. The electrochemical behaviour of these modified electrodes were examined in $[Fe(CN)_6]^{3-/4-}$, $[Ru(NH_3)_6]^{2+/3+}$ and ferrocene.

3.3. SEM characterization of modified EG electrodes

The modified electrodes were first characterized using SEM to confirm the deposition of the nanoparticles onto the electrode surfaces. The electrodeposition of PPI onto the EG (EG-PPI) was noted by the smooth surface under the scanning electron microscope (Figure 4a) due to the elemental components of the dendrimer. However, EG-PPI-AuNP (Figure 4b) showed an even distribution of AuNP and a uniform size (less than 50 nm) distribution which was effected by the presence of PPI dendrimer. This is because the PPI formed caps around each AuNP causing uniform dispersion resulting in a controlled particle size despite the electrodeposition method being the same, a behaviour which was also reported by Arotiba *et al* [12]. In the absence of PPI, the gold fully covered the EG surface as shown by the colour lightening of the surface in Figure 4c (and also a prominent gold colour on visual inspection) compared to Figure 4b.

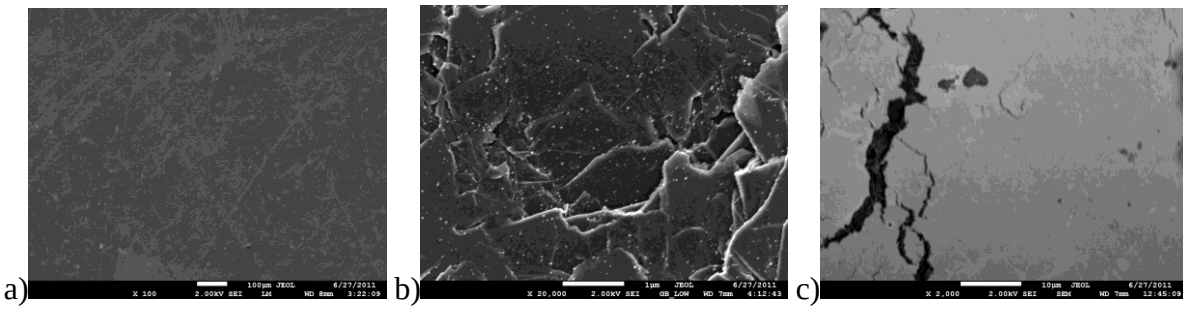

Figure 4. SEM images of a) EG-PPI b) EG-PPI-AuNP c) EG-AuNP electrodes.

3.4. Electrochemical characterization of EG and modified EG in $[Fe(CN)_6]^{3-/4-}$, $[Ru(NH_3)_6]^{2+/3+}$ and ferrocene redox systems

The values of ΔE and E°′ (formal potential) obtained from the cyclic voltammograms of the three redox systems using the bare and modified EG and GCE electrodes are listed in Table 3 below.

Table 3. The potential peak separation (ΔE in mV), formal potentials (E°′ in mV) and peak current (I_{pa} in μA) of the redox peaks obtained from the CVs of $[Fe(CN)_6]^{3-/4-}$, $[Ru(NH_3)_6]^{2+/3+}$ and ferrocene on the bare and modified EG electrodes.

	$[Fe(CN)_6]^{3-/4-}$			$[Ru(NH_3)_6]^{2+/3+}$			Ferrocene		
	ΔE	E°	I_{pa}	ΔE	E°	I_{pa}	ΔE	E°	I_{pa}
GCE	90	227.0	84.2	74	-139.5	17.7	97	427.0	92.6
GCE-PPI	93	221.5	89.8	74	-138.5	19.3	112	428.0	102.3
GCE-AuNP	92	220.5	89.4	71	-136.0	20.4	89	433.5	99.4
GCE-PPI-AuNP	90	219.5	92.5	69	-135.5	21.9	86	426.0	101.7
EG	113	241.5	90.6	85	-152.5	26.4	107	425.5	112.2
EG-PPI	116	235.0	135.9	97	-150.5	31.3	107	427.0	124.5
EG-AuNP	109	233.5	122.6	84	-147.0	29.4	113	423.5	120.9
EG-PPI-AuNP	108	230.5	105.9	84	-144.0	28.1	105	420.5	116.8

In general, the modified electrodes resulted in higher peak currents than the bare electrodes as shown in Figure 5. This is attributed to the nano-structured and conducting nature of the modifiers which increased the effective surface area and improved the conductivity of the EG electrode respectively [14,30]. Furthermore, the possible catalytic effects of the nanomaterials also contribute to the varied electrochemical responses observed. The effects of modification can be noticed based on the variation of the recorded peak currents, potential peak separation and formal potential. This suggests that the EG electrode easily lends itself to modification and its properties can be tuned based on the modifier used.

In the CV of 5 mM $[Fe(CN)_6]^{3-/4-}$ redox system (Figure 5), all the electrodes showed well defined quasi-reversible redox peaks. The EG-PPI electrode gave the highest anodic and cathodic peak currents for both the anodic and cathodic peaks despite the fact that it had the highest ΔE value. The high peak currents recorded (more pronounced in SWV shown in Figure 5c) is attributed to a higher surface area available for the interfacial electrochemistry of the redox probe as a result of the attached PPI dendrimer. PPI dendrimers have interior voids which add to the porous character of EG and thus affecting the rate of electron transfer when compared to the metallic nanoparticles-modified EG electrodes. Similar responses were observed for EG-PPI in the $[Ru(NH_3)_6]^{2+/3+}$ and ferrocene redox systems as illustrated in Table 3.

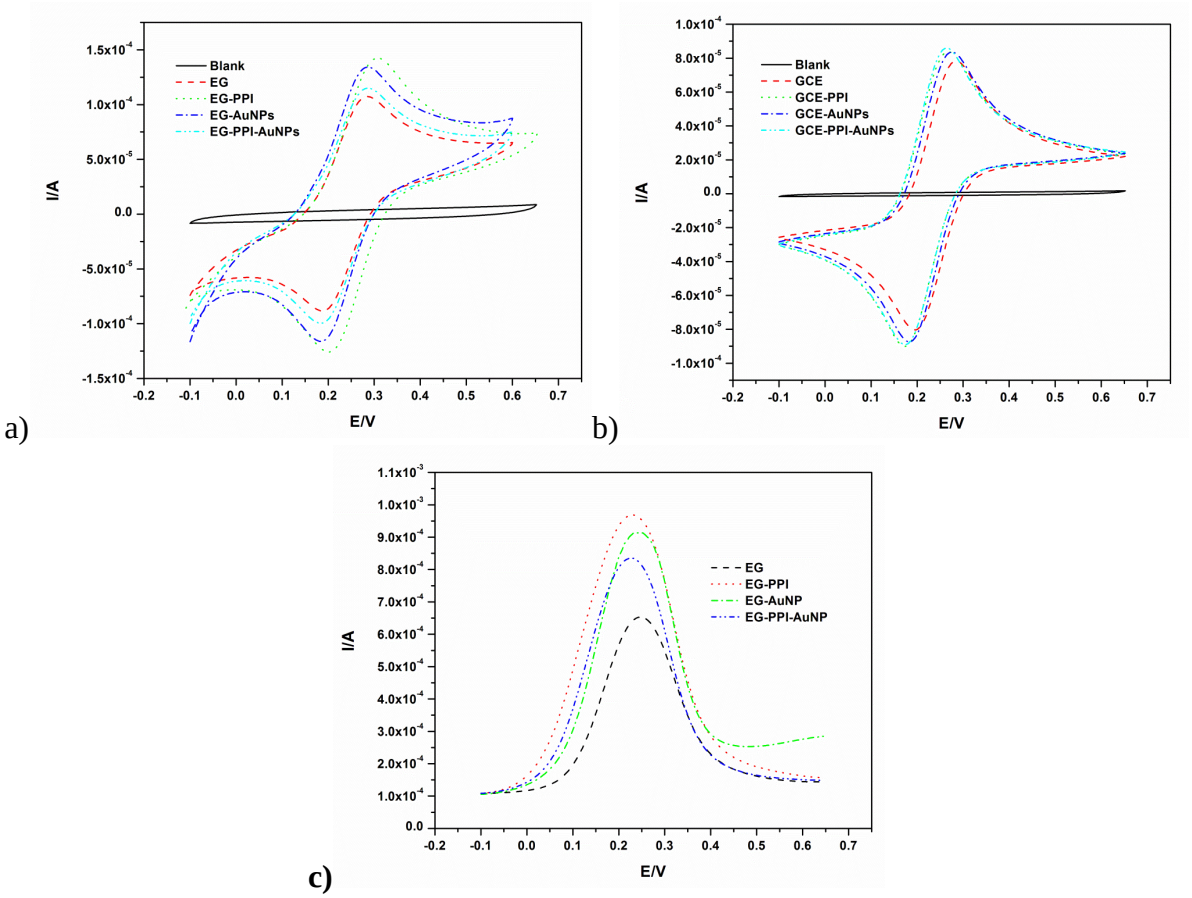

Figure 5. CVs of all the modified electrodes in 5 mM $[Fe(CN)_6]^{3-/4-}$ at **a)** the EG electrode and **b)** the GCE. The CVs were recorded at a scan rate of 50 mV/s. **c)** shows the corresponding SWVs in 5 mM $[Fe(CN)_6]^{3-/4-}$ recorded on the EG based electrodes at amplitude 50 mV and a frequency of 25 Hz.

The reversibility of an electrochemical reaction (defined in terms of peak potential separation, ΔE) is highly influenced by the nature of the electrode material. It can be said that the lower the value of ΔE of a system, the higher its reversibility. This means that the EG-PPI-AuNP platform allows for better reversibility (faster electron kinetics) in $[Fe(CN)_6]^{3-/4-}$, $[Ru(NH_3)_6]^{2+/3+}$ and ferrocene redox systems compared to the unmodified electrode (Table 3). The combination of PPI and AuNP is seen to have beneficial kinetic effects on the EG electrode relative to using these modifiers individually.

EG-AuNP consistently gave higher currents and better reversibility than the EG electrode in all the redox systems used (Table 3 and Figure 5 showing that of $[Fe(CN)_6]^{3-/4-}$ only). AuNP have found extensive usage in electrochemistry as matrices for the immobilization of macromolecules like proteins, enzymes and antibodies [12,31]. They assist in constructing an interface for direct electron transfer of active proteins while retaining their bioactivity as they provide a natural environment allowing for longer life stability [12]. These AuNP properties combined with the proposed electrocatalytic property of PPI dendrimer [18,25] are responsible for the observed behaviour of the EG-PPI-AuNP, EG-PPI and EG-AuNP electrodes. The PPI dendrimer as well as the PPI-AuNP have been successfully used as a DNA biosensor platform [18,32].

Evidence of good reversibility of $[Ru(NH_3)_6]^{2+/3+}$ was observed in the values of ΔE obtained for all the modified and bare electrodes which were all below 97 mV on the EG electrode (Table 3). This behavior was consistent as the low ΔE values were also obtained from the modified GCE. Even though the GCEs showed better reversibility in all the redox systems, the behavior of the bare and modified EG electrodes was also satisfactory. This suggests that the EG electrode can be explored for use in areas such as in the electroanalysis of various environmental and biological molecules, where the GCE is also favoured.

The experiments were repeated three times on the same electrode and on fresh electrodes with RSD values less than 4.3% for both the peak currents and potentials. This implies that the EG electrode can be a reliable electrode material which gives reproducible results. The electrode surface was polished using emery paper with a fine grid of 1600 followed by polishing on a weighting paper to obtain a smooth surface - the lubricating nature of EG aids in easy electrode surface renewal. This step results in the removal of the top graphitic layer, leaving a fresh clean surface.

4. CONCLUSION

This work has shown that exfoliated graphite (EG) electrode can be used as a cheaper electrode substitute to GCE owing to similar and sometimes better electrochemical properties possessed by EG. Furthermore, characteristics such as ease of fabrication, amenability to modification, and surface renewal after cleaning (thus eliminating interference from any surface adsorbed specie) may be seen as advantages of EG over GCE. The application of EG electrode in lieu of other carbon based electrodes for electroanalysis may be a worthwhile alternative for electrochemists.

ACKNOWLEDGMENTS

The authors would like to thank the University of Johannesburg, Nanotechnology Innovation Centre (NIC), National Research Foundation (NRF) and Council of Scientific and Industrial Research (CSIR) for funding this project.

References

1. B.K. Jena and C.R. Raj, *Talanta*, 76 (2008) 161
2. A. Salimi, H. Mamkhezri, R. Hallaj, and S. Soltanian, *Sensor. Actuator. B: Chem.*, 129 (2008) 246
3. N.Y. Stojko, K.Z. Brainina, C. Faller, and G. Henze, *Anal. Chim. Acta*., 371 (1998) 145
4. D.D.L. Chung, *J. Mater. Sci*., 22 (1987) 4190
5. D.D.L. Chung, *J. Mater. Sci*., 37 (2002) 1475
6. P. Ramesh and S. Sampath, *Chem. Commun*., 21 (1999) 2221
7. C. Frysz and D.D.L. Chung, *Carbon*, 35 (1997) 858
8. P. Monk, Fundamentals of Electro-Analytical Chemistry, John Wiley & Sons LTD, Manchester, UK (2005).
9. SPI® Supplies, Brand Glassy (Vitreous) Carbon Products, 'Glassy Carbon 1.' Available at: http://www.2spi.com/catalog/mounts/vitreous.php (Access date 02 September 2011).
10. P. Ramesh and S. Sampath, *Anal. Chem*., 75 (2003) 6949

11. R. Chai, R. Yuan, Y. Chai, C. Ou, S. Cao, and X. Li, *Talanta*, 74 (2008) 1330
12. X. Dai and R.G. Compton, *Electroanalysis*, 17 (2005) 1325
13. A. Salimi, R. Hallaj, S. Soltanian, and H. Mamkhezri, *Anal. Chim. Acta*., 594 (2007) 24
14. M.-G. Li, Y.-J.Shang, Y.-C.Gao, G.-F. Wang, and B. Fang, *Anal. Biochem*., 341 (2005) 52
15. S. Xing, H. Xu, J. Chen, G. Shi, and L. Jin, *J. Electroanal. Chem*., 652 (2011) 60
16. M. Yang and Z. Hu, *J. Electroanal. Chem*., 583 (2005) 46
17. R.O. Kadara, N. Jenkinson, and C.E. Banks, *Electroanalysis*, 21 (2009) 2410
18. O.A. Arotiba, J.H. Owino, P.G. Baker, and E.I. Iwuoha, *J. Electroanal. Chem*., 638 (2010) 287
19. O.A. Arotiba, E.A. Songa, P.G. Baker, and E.I. Iwuoha, *Chemistry Today*, 27 (2009) 55
20. G.-ho Hwang, W.-kyu Han, S.-jun Hong, J.-shik Park, and S.-goon Kang, *Talanta*, 77 (2009) 1432
21. I. Švancara, L. Baldrianová, E. Tesařová, S.B. Hočevar, S.A.A. Elsuccary, A. Economou, S. Sotiropoulos, B. Ogorevc, and K. Vytřas, *Electroanalysis*, 18 (2006) 177
22. X. Luo, A. Morrin, A.J. Killard, and M.R. Smyth, *Electroanalysis*, 18 (2006) 319
23. M. Bonnissel, L. Luo, and D. Tondeur, *Carbon*, 39 (2001) 2151
24. A. Celzard, J.F. Mareche, and G. Furdin, *Prog. Mater. Sci*., 50 (2005) 93
25. T. Ndlovu, O.A. Arotiba, S. Sampath, R.W. Krause, and B.B. Mamba, *J. Appl. Electrochem*., 41 (2011) 1389
26. P.R. Unwin, Introduction to Electroanalytical Techniques and Instrumentation, University of Warwick, Coventry, UK.
27. C.A. Frysz, X. Shui, and D.D.L. Chung, *Carbon*, 35 (1997) 893
28. D. Salinas-torres, F. Huerta, F. Montilla, and E. Morallón, *Electrochim. Acta*, 56 (2011) 2464
29. S.A. Wring and J.P. Hart, *Analyst*, 117 (1992) 1215
30. B. Rezaei and S. Damiri, *Talanta*, 83 (2010) 197
31. T. Tangkuaram, C. Ponchio, T. Kangkasomboon, P. Katikawong, and W. Veerasai, *Biosens. & bioelectron.*, 22 (2007) 2071
32. O.A. Arotiba, P.G. Baker, B.B. Mamba, and E.I. Iwuoha, *Int. J. Electrochem. Sci*., 6 (2011) 673